Clim Dyn (2018) 50:1733–1745
DOI 10.1007/s00382-017-3718-6

Tree-ring stable carbon isotope-based April–June relative humidity reconstruction since AD 1648 in Mt. Tianmu, China

Yu Liu[1,3,4] · Weiyuan Ta[1,2,5] · Qiang Li[1] · Huiming Song[1] · Changfeng Sun[1,4] · Qiufang Cai[1] · Han Liu[1,2] · Lu Wang[1,2] · Sile Hu[1,2] · Junyan Sun[1] · Wenbiao Zhang[6] · Wenzhu Li[6]

Received: 21 December 2016 / Accepted: 1 May 2017 / Published online: 12 May 2017

Abstract Based on accurate dating, we have determined the stable carbon isotope ratios ($\delta^{13}C$) of five *Cryptomeria fortunei* specimens from Mt. Tianmu, a subtropical area in southern China. The five $\delta^{13}C$ time series records are combined into a single representative $\delta^{13}C$ time series using a "numerical mix method." These are normalized to remove temporal variations of δ^{13} C in atmospheric CO_2 to obtain a carbon isotopic discrimination ($\Delta^{13}C$) time series, in which we observe a distinct correlation between $\Delta^{13}C$ and local April to June mean relative humidity ($\boldsymbol{RH}_{\mathbf{AMJ}}$) (n = 64, $r = 0.858$, $p < 0.0001$). We use this relationship to reconstruct $\boldsymbol{RH}_{\mathbf{AMJ}}$ variations from AD 1648 to 2014 at Mt. Tianmu. The reconstructed sequence show that over the past 367 years, Mt. Tianmu area was relatively wet, but in the latter part of the twentieth century, under the influence of increasing global warming, it has experienced a sharp reduction in relative humidity. Spatial correlation analysis reveals a significant negative correlation between $\boldsymbol{RH}_{\mathbf{AMJ}}$ at Mt. Tianmu and Sea Surface Temperature (SSTs) in the western equatorial Pacific and Indian Ocean. In other words, there is a positive correlation between tree-ring $\delta^{13}C$ in Mt. Tianmu and SSTs. Both observed and reconstructed $\boldsymbol{RH}_{\mathbf{AMJ}}$ show significant positive correlations with East Asian and South Asian monsoons from 1951 to 2014, which indicate that $\boldsymbol{RH}_{\mathbf{AMJ}}$ from Mt. Tianmu reflects the variability of the Asian summer monsoon intensity to a great extent. The summer monsoon has weakened since 1960. However, an increase in relative humidity since 2003 implies a recent enhancement in the summer monsoon.

Keywords Mt. Tianmu, China · *Cryptomeria fortunei* · Tree-ring $\delta^{13}C$ · Relative humidity · Asian summer monsoon

1 Introduction

Quantifying the nature of ongoing climate change is an imperative concern in today's world. Paleoclimatic time series records from around the globe are necessary to fully understand past climate change and more recent anthropogenic impacts (Jones and Mann 2004). The acquisition of high-resolution paleoclimate data is of special significance for understanding climate change as a means of testing and improving climate models, and improving the accuracy and reliability of model-based predictions. However, the instrumental climate record is currently very limited and far from meeting the needs for detailed climate change simulations. Among the various geological and biological

Electronic supplementary material The online version of this article (doi:10.1007/s00382-017-3718-6) contains supplementary material, which is available to authorized users.

✉ Yu Liu
liuyu@loess.llqg.ac.cn

[1] The State Key Laboratory of Loess and Quaternary Geology, Institute of Earth Environment, Chinese Academy of Sciences, Xi'an 710061, China

[2] University of Chinese Academy of Science, Beijing 100049, China

[3] Joint Center for Global Change Studies (JCGCS), Beijing Normal University, Beijing 100875, China

[4] Department of Environmental Science and Technology, School of Human Settlements and Civil Engineering, Xi'an Jiaotong University, Xi'an 710049, China

[5] Shaanxi Appraisal Center for Environmental Engineering, Xi'an 710065, China

[6] Zhejiang Agriculture and Forestry University, Zhejiang 311300, China

proxies available for detailed climatic reconstruction, tree rings have several significant advantages, including: dating accuracy, high resolution, temporal continuity, and wide geographic availability (Mann et al. 2008; Cook et al. 2010; Sano et al. 2009; Liu et al. 2010a, b, 2012b, 2015).

Tree ring studies contain a number of well-known climate proxies. Among these, stable carbon isotope records ($\delta^{13}C$) have unique advantages, such as known fractionation mechanisms, high signal/noise ratios and good preservation of the low-frequency signals (Leavitt and Lone 1989a, b; Gagen et al. 2011; Treydte et al. 2009; McCarroll and Loader 2004; Liu et al. 2012a, 2014). Stable carbon isotope records are especially useful for paleoclimate studies in regions where climatic characteristics are not captured well by conventional tree-ring width and density studies (Loader et al. 2011; Liu et al. 2007).

In China, the relation between tree-ring $\delta^{13}C$ and climate has been explored in some detail, and tree-ring $\delta^{13}C$ has been shown to be an effective proxy to reconstruct temperature (Liu et al. 2007, 2012a, 2014), precipitation (Wang et al. 2001; Liu et al. 2003), the Palmer drought severity index (Liu et al. 2010a, b), water use efficiency (Xu et al. 2013), and rainfall intensity in the marginal monsoon zones (Liu et al. 2008). This research has greatly promoted the development of dendroclimatology in China.

In this study, we selected Mt. Tianmu as a representative of a sub-tropical forest in southern China to establish a relationship between tree-ring $\delta^{13}C$ and climate, following strict dendrochronological methodologies. We have reconstructed April to June relative humidity values in the region, with more than 300 years of continuous coverage. These results provide a reference for further tree ring research and climate reconstruction in warm and humid regions. Previous studies from the region showed relationships between tree-ring $\delta^{13}C$ and climatic factors. For example, precipitation and winter temperature signals were found by using two trees (Qian et al. 2002, 1832–1997, 1833–1983), and an August to September maximum temperature was reconstructed using one tree (Zhao et al. 2014, 1685–1985). However, for tree-ring isotopic study, at least four trees are needed (Leavitt and Long 1984). In another aspect, these $\delta^{13}C$ time series ended too early to show the variation trends in the recent two decades. It is, therefore, necessary to study additional samples from the region to make a comprehensive assessment of the relationship between stable isotopes and climate in a context of global changes over recent decades.

Relative humidity (***RH***) is the ratio of water vapor pressure in air to its saturated water vapor pressure at a given air temperature. Existing research shows that relative humidity is a dominant factor in the control of interannual tree-ring $\delta^{13}C$ changes (Saurer et al. 1997). Higher relative humidity would result in higher humidity in air in the region and an increased likelihood of flooding, and vice versa. Accordingly, it is imperative to research long-term changes in relative humidity.

2 Materials and methods

2.1 Sampling

Mt. Tianmu (119°24′11″E–119°28′21″E, 30°18′30″N–30°24′55″N), climbs steeply from an altitude of about 300 m to more than 1550 m, near Linan City, Zhejiang Province (Fig. 1). The mountain has relatively high humidity year-round, under a subtropical warm and humid monsoon climate (Zhao et al. 2005), with a range in relative humidity from 67.0% in winter to 89.0% in summer. The mean annual temperature is 8.86 °C, with a January mean air temperature of −2.5 °C and a July mean temperature of 20.0 °C. Mean annual rainfall is 1419.8 mm (1956–1997, Tianmushan Meteorological Station).

Mt. Tianmu features a complex vegetation distribution, with vertical zonation according to elevation. The sampling area is primarily covered with *Cryptomeria fortunei*, and *Hooibrenkex Ottoet Dietr*. Thirty-two trees were sampled at Mt. Tianmu for this study, from which 80 tree cores were obtained, including 9 trees with 3 replicate cores each (A-core, B-core, C-core). The samples were taken back to the laboratory for cross-dating, based on the A-core and B-core of all trees, using standard tree-ring research protocols (Cook and Kariukstis 1990; Stokes and Smiley 1996) for built width chronology to ensure definitive calendar ages for every growth ring. The ring-width chronology for Mt. Tianmu covers the period 1618–2014 AD. Statistical characteristics of the standard chronology are shown in the Supplementary Table S1.

2.2 Extraction of α-cellulose and construction of a $\delta^{13}C$ time series

Generally speaking, ring width and core longevity should be considered for stable isotope analysis (Porter et al. 2014; Leavitt et al. 2010). Therefore, we selected C-cores from five trees with relatively long-lived, wide growth rings and fewer absent rings for analysis of stable carbon isotopes. The C-cores from five trees were systematically peeled off from their most outer layer ring under magnification. Every ring was sampled and placed into test tubes, and numbered according to age. The longest sample is 397 years. To accurately document $\delta^{13}C$ changes in the tree rings, we removed lignin and hemi-cellulose. The cellulose was homogenized by an ultrasonic cell pulverizer, using the Jayme-Wise procedure (Leavitt and Long 1984; Stuiver et al. 1987; Liu et al. 1996, 2012a, 2014). The detailed steps are as follows:

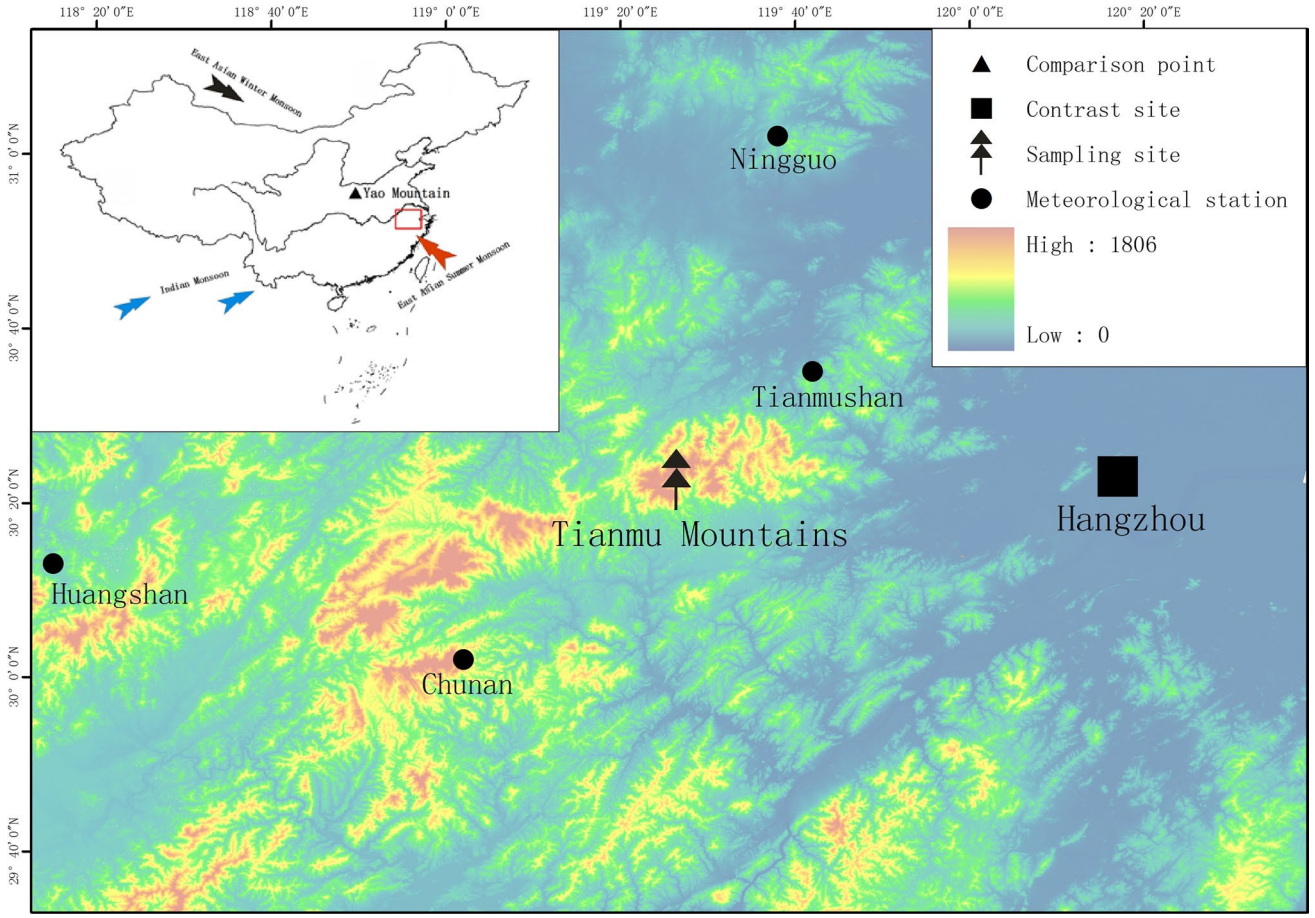

Fig. 1 Map showing the sampling site and the meteorological station nearby (the monsoon route is from An et al. 2006)

(1) soak the sliced sample in 200 ml of mixed solution composed of benzene and alcohol (2:1); (2) dip into acetone; (3) add sodium chlorite ($NaClO_2$) and acetic acid until the sample turns white in color to obtain holocellulose; (4) repeatedly soak into 17.5% sodium hydroxide (NaOH) 3 times and rinse thoroughly until neutral; (5) soak into acetic acid and rinse thoroughly until neutral. The α-cellulose is then homogenized and freeze-dried.

The procedure used to determine $\delta^{13}C$ in α-cellulose was as follows: (1) a FLASH 2000 elemental analyzer and dynamic combustion unit was used to oxidize the carbon to CO_2; (2) the CO_2 was transferred to a DELTA V ADVANTAGE isotope ratio mass spectrometer to measure $^{13}C/^{12}C$ ratios. One standard cellulose sample (IAEA CH3, 24.724‰) was inserted for every 7 samples. The 0.2‰ of measurement was obtained by repeated measurement of IAEA CH3. All determinations were completed in the State Key Laboratory of Loess and Quaternary Geology, Chinese Academy of Sciences.

The tree ring carbon isotope ratio of cellulose is quoted as $\delta^{13}C$ values (Coplen 1995):

$$\delta^{13}C = (R_{\text{sample}} / R_{\text{standard}} - 1) \times 1000‰ \quad (1)$$

where $R = {}^{13}C/{}^{12}C$ and R_{sample} and R_{standard} are the sample and standard measured ratios, respectively.

$\delta^{13}C$ time series of C-cores of five trees are indicated by TM1-TM5 respectively, and the five time series are incorporated into the main $\delta^{13}C$ time series TM_com, a representative $\delta^{13}C$ time series of Mt. Tianmu, obtained by the numerical mix method (Liu et al. 2012a, 2014). Statistical characteristics of every single $\delta^{13}C$ series of α-cellulose and composite $\delta^{13}C$ are shown in Table 1. The average value of every $\delta^{13}C$ series ranges from −22.97 to −21.25‰. Generally speaking, this is identical with previous research of $\delta^{13}C$ in Chinese pine in Helan Mountain and the Huangling region in Shaanxi Province (Liu et al. 1996, 2004). During the common period of 5 cores (1848–1976), the statistical features of composite series are shown in Table 2.

Since the juvenile effects in trees (Freyer 1979; Leavitt and Long 1984; Liu et al. 1996, 2012b; Hou et al. 2001; Szymczak et al. 2012) are likely to enrich $\delta^{13}C$ values from

Table 1 Statistical characteristics of the α-cellulose $\delta^{13}C$ time series of Mt. Tianmu

Parameter	TM1	TM2	TM3	TM4	TM5	TM_com
Minimum value	−23.66‰	−24.53‰	−23.41‰	−23.69‰	−24.57‰	−23.66‰
Maximal value	−19.86‰	−20.73‰	−19.35‰	−20.64‰	−20.65‰	−20.18‰
Mean value	−21.35‰	−21.81‰	−21.25‰	−22.20‰	−22.97‰	−21.66‰
AR1	0.63	0.49	0.65	0.75	0.68	0.56
AR2	0.56	0.49	0.55	0.62	0.55	0.52
AR3	0.47	0.45	0.50	0.55	0.51	0.41
Sequence length	392	337	363	167	172	397
Start and end year	1618–2013	1637–1976	1625–2014	1847–2014	1838–2014	1618–2014
Standard deviation	±0.64	±0.56	±0.62	±0.61	±0.64	±0.57
Skewness	−0.53	−1.02	−0.18	−0.08	0.37	−0.41
Kurtosis	0.37	2.19	−0.06	−0.36	1.17	0.31

Table 2 Statistical characteristics of the $\delta^{13}C$ composite time series during common interval (1848–1976)

Statistical term	Statistic
Mean value	–21.7‰
Standard deviation	±0.57‰
Skewness	0.47
Kurtosis	0.36
Mean sensitivity	0.15
Signal-to-noise ratio	3.22
Mean correlation within series	0.53
Autocorrelation	
AR1	0.72
AR2	0.30
AR3	0.12

close-to-core tree rings (Leavitt and Long 1984; Freyer 1979), it is necessary to remove the interference of juvenile effects. Among the 5 sample cores analyzed here, TM4 and TM5 have abandoned samples about 30 years close to the core in the sample peeling, while TM1, TM2, and TM3 contain core rings. After consideration, we removed the data of TM1, TM2, and TM3 from the first 30 years to eliminate any potential juvenile effects in the $\delta^{13}C$ record. With the elimination of juvenile effects, the statistical correlation between the individual time series of $\delta^{13}C$ in Mt. Tianmu is shown in Table 3

We noticed the relatively negative $\delta^{13}C$ values of TM5, but its explanation is difficult. It may be caused by different standing conditions. However, the variation in $\delta^{13}C$ of the TM5 series is synchronous with the other 4 cores (Table 2; Fig. 2a). Previous studies have shown that there is no absolute reference value for comparison, so we have used the mean of several trees as the true value (Leavitt et al. 1984). The between-tree variability in the absolute isotopic ratios is a significant but surmountable problem, and more sample size in generating the final composite is a good way to solute this problem (McCarroll and Loader 2004)

There is significant correlation among the five time series, with significant first-order autocorrelation (AR1) of 5 single series and composite series, indicating that there is a significant isotope lag effect from the previous year to the present year, in both the single series and composite series, and significant correlation between the individual $\delta^{13}C$ time series. In particular, the correlation coefficients between the composite series and single series are greater than 0.7, indicating that the composite series effectively captures $\delta^{13}C$ variations in growth rings of local trees (Fig. 2a).

Our tree-ring $\delta^{13}C$ composite showed a significantly increasing trend in recent decades (Fig. 2a), consistent with a previous study that is 17 years shorter than ours, in the

Table 3 Statistical correlation between the $\delta^{13}C$ and $\Delta^{13}C$ time series

		$\delta^{13}C/\Delta^{13}C$				
		TM1	TM2	TM3	TM4	TM5
$\delta^{13}C/\Delta^{13}C$	TM1					
	TM2	0.50/0.39				
	TM3	0.68/0.70	0.49/0.36			
	TM4	0.48/0.68	0.68/0.55	0.50/0.71		
	TM5	0.57/0.59	0.39/0.22	0.48/0.51	0.38/0.60	
	TM_com	0.79/0.80	0.72/0.61	0.80/0.81	0.75/0.90	0.74/0.76

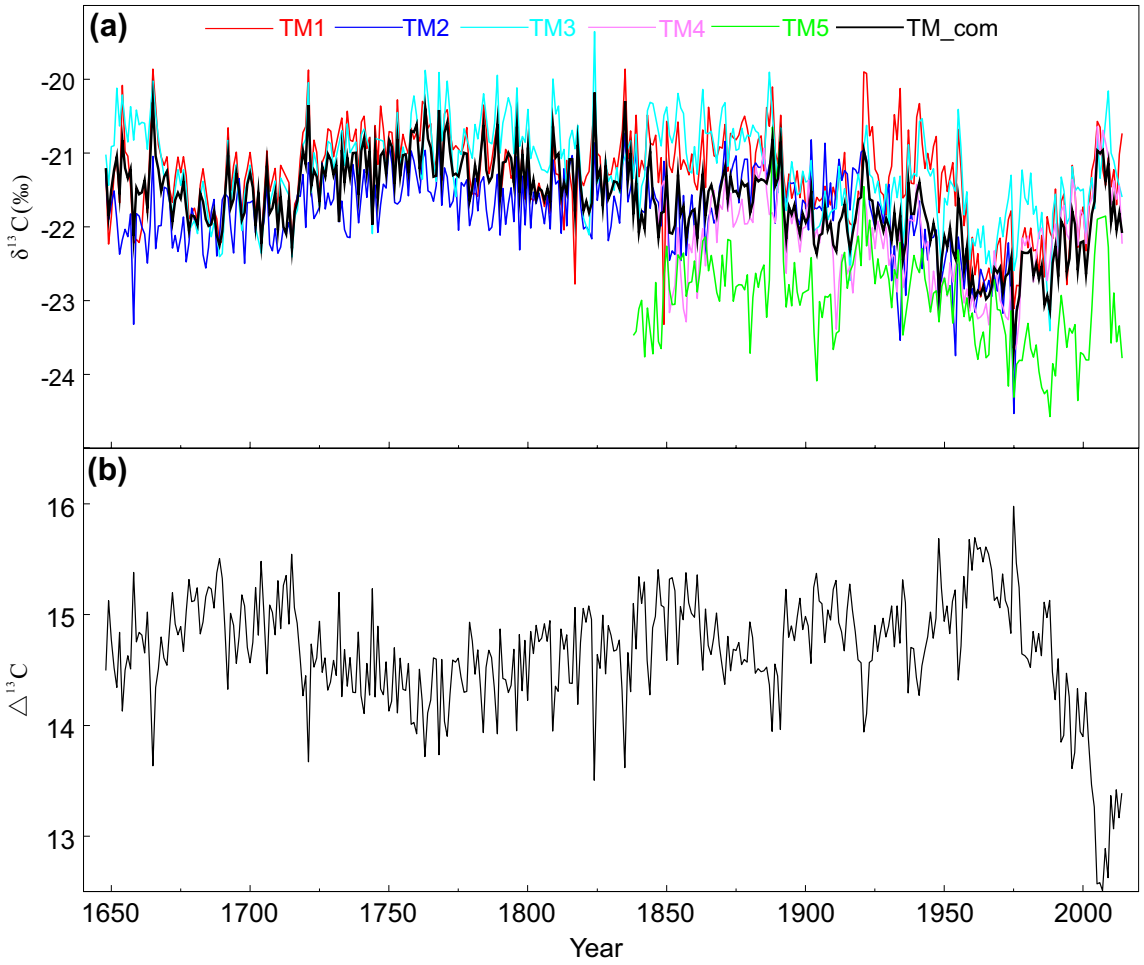

Fig. 2 **a** Single and composite $\delta^{13}C$ time series (with 30 years of juvenile growth removed); **b** composite Mt. Tianmu $\Delta^{13}C$ time series

region that the $\delta^{13}C$ series had shown an increasing trend from 1975 to 1997 (Zhao et al. 2014).

A large amount of isotopically "light" carbon has been emitted into the atmosphere due to the use of fossil fuels since the start of the industrial revolution. This has been sufficient to decrease $\delta^{13}C$ values in atmospheric CO_2 and in plants (McCarroll and Loader 2004; McCarroll et al. 2009). Therefore, to understand climatic effects in tree ring $\delta^{13}C$ records, it is necessary to filter out the anthropogenic imprint of fossil fuels (McCarroll and Loader 2004).

Adopting the approach developed in the study of $\delta^{13}C$ ratios from CO_2 in ice core bubbles (McCarroll and Loader 2004) to δ^{13} C of atmospheric CO_2, we obtained a normalized carbon isotope fractionation time series (Carbon Isotopic Discrimination, Δ). Δ is defined as:

$$\Delta = \left(\delta^{13}C_{air} - \delta^{13}C_{tree}\right)/\left(1 - \delta^{13}C_{tree}/1000\right) \quad (2)$$

where $\delta^{13}C_{\mathrm{air}}$ is the $\delta^{13}C$ value of CO_2 in the atmosphere, and $\delta^{13}C_{\mathrm{tree}}$ is the measured $\delta^{13}C$ value determined in tree ring cellulose.

This value serves to remove atmospheric variations in the $\delta^{13}C$ time series that are unrelated to climate. We observe that all five of our individual $\Delta^{13}C$ time series and our composite $\Delta^{13}C$ time series show significant correlation (Table 3). This indicates that these chronologies share a common high frequency signal, and the composite $\Delta^{13}C$ time series record captures changes in the individual tree ring time series. Figure 2b shows the composite tree-ring time series of $\Delta^{13}C$ in Mt. Tianmu. We examine the implications of our $\Delta^{13}C$ time series in terms of climate in the following discussion.

3 Climate data

We selected a 64-year meteorological record from the Hangzhou station (120°17′E, 30°23′N, altitude: 43.2 m, 1951–2014), which is located in the same climatic region and incurs no data loss.

Prior to the study, we perfomed homogeneity and mutation tests (Potter 1981; Peterson and Easterling 1994; Easterling and Peterson 1995) on the records, selecting four meteorological stations as references, including Tianmushan (119°42′E, 30°35′N, altitude: 1502.9 m, 1956–1997), Chunan (119°02′E, 29°62′N, altitude: 172.2 m, 1998–2014), Ningguo (118°98′E, 30°62′ N, altitude: 89.0 m, 1956–2014) and Huangshan (118°15′E, 30°13′N, altitude: 1836.3 m, 1956–2014). The results of the homogeneity and mutation tests indicate that the meteorological data at the point are true and reliable, and are suitable for detailed study.

We note that there exit discrepancies of ***RH*** between the Tianmushan (nearest to our sampling site) and Hangzhou station (Xu et al. 2016), which may be caused by a different geographic location (e.g., altitude, plain/forest). However, the ***RH*** record of the Tianmushan station is much shorter (42 years) than that of the Hangzhou station (64 years). The Tianmushan records only extend to 1998, with incomplete coverage in some years. More importantly, the decreasing trend in relative humidity (***RH***), which is discussed below, recorded in nearby stations in large scale, was not observed at the Tianmushan station.

We used the meteorological data from China Integrated Meteorological Information Service System (CIMISS, http://data.cma.cn). The monthly mean temperature, precipitation and relative humidity at the Hangzhou meteorological station are shown in Fig. 3a. The mean annual precipitation is 1421.7 mm and the precipitation reaches a maximum in June. The monthly mean temperature peaks in July and August, and the annual average relative humidity is 77.4%, with 2 peaks in June and September.

4 Correlation between $\Delta^{13}C$ and climatic factors

To ascertain the representative significance of the composite Tianmu $\Delta^{13}C$ time series in terms of climate, we apply Pearson correlation functions to assess the covariance between the $\Delta^{13}C$ time series and primary climatic factors (average temperature, precipitation, and relative humidity) from the Hangzhou Meteorological Station (Fig. 4a). Temperature and relative humidity are the main climatic factors that appear to influence tree ring $\delta^{13}C$. The temperature relationship is expressed as a negative correlation between $\Delta^{13}C$ of tree ring and temperature from the previous August

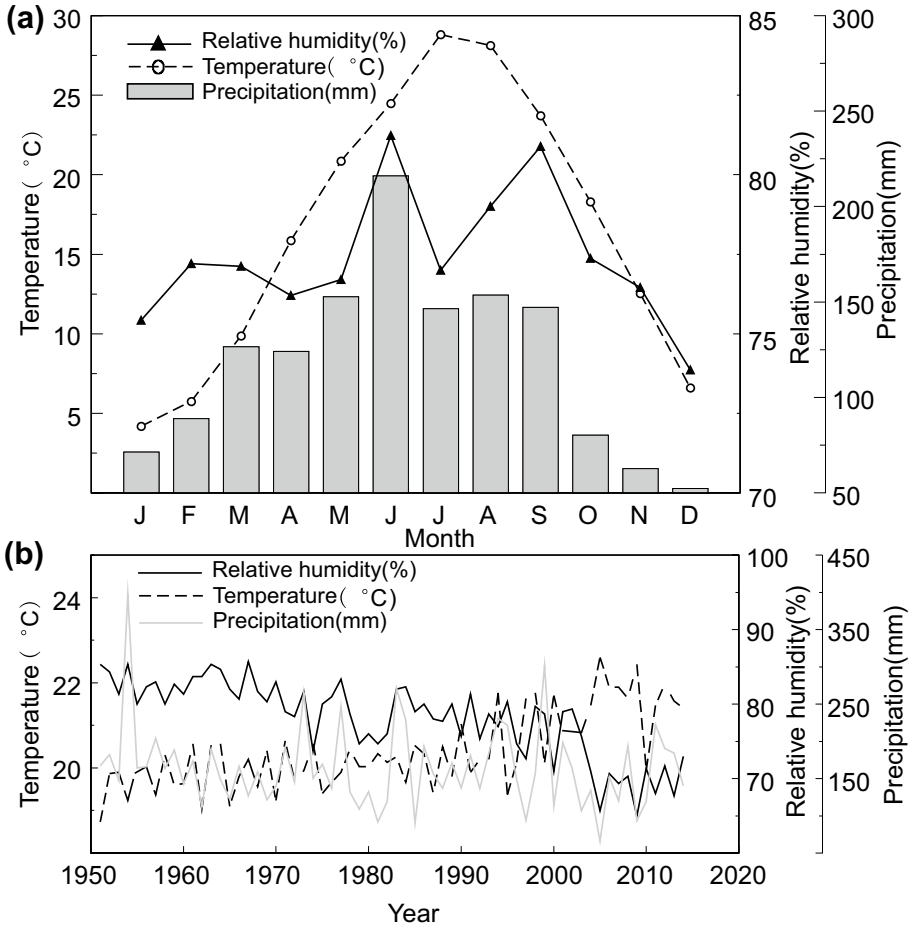

Fig. 3 **a** Monthly mean temperature, precipitation and relative humidity at the Hangzhou Meteorological Station (1951–2014); **b** mean temperature, precipitation and relative humidity from April to June in the Mt. Tianmu region

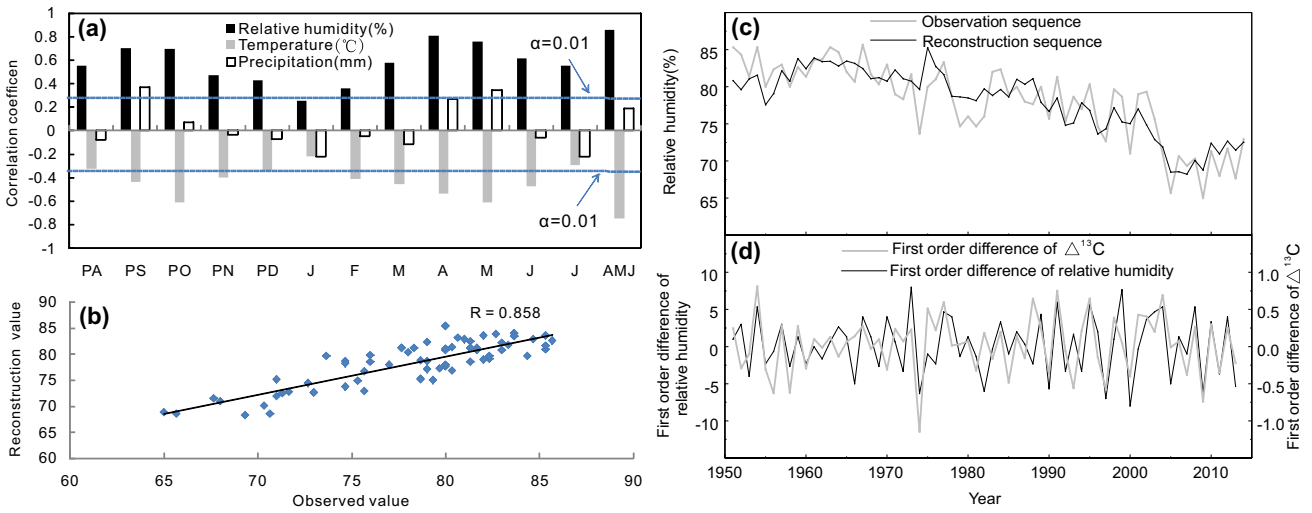

Fig. 4 **a** Correlation between the $\Delta^{13}C$ time series and monthly mean temperature, monthly relative humidity, monthly precipitation during 1951–2014 AD; **b** scatter diagram of the correlation between the observed and estimated mean relative humidity (April–June, 1951–2014); **c** comparison of reconstructed and observed mean relative humidity sequence from April to June during the period 1951–2014 AD at Mt. Tianmu; **d** comparison of first-order difference sequence

to July of this year, while relative humidity is positively correlated with tree ring $\Delta^{13}C$ for every month during this period. In addition, there is significant correlation between tree ring $\Delta^{13}C$ and temperature from August to October of the previous year and from the growing season March to July of the current year. Figure 4a shows that higher relative humidity values would result in higher $\Delta^{13}C$ values, and vice versa. There is an inverse correlation between local temperature and relative humidity (Fig. 3b). Consequently, the observed inverse correlation with temperature given in Fig. 4a is reasonable.

The above results also conforms to known $\delta^{13}C$ isotopic fractionation mechanisms in plant cellulose (Farquhar et al. 1982). There is a reasonable physiological explanation. As *Cryptomeria fortunei* absorbs CO_2 through foliage, and in the case that relative humidity is higher in the growing season (lower temperature), the foliar surfaces will open wider and thus absorb more CO_2 into the foliage for photosynthesis. Lighter carbon atoms (^{12}C) escape from within the foliage by transpiration, leaving a higher proportion of ^{13}C behind, therefore enriching the ^{13}C content of the foliage.

The growing season of *Cryptomeria fortunei, Hooibrenkex Ottoet Dietr* is from April to October (Jiang et al. 2012). After a combination of months, we find that the correlation with mean relative humidity ($\boldsymbol{RH}_{\mathbf{AMJ}}$) in the growing season, from April to June, is 0.86 (n = 64, $p < 0.0001$) (Fig. 4b) and the correlation with mean temperature from April to June is 0.75 (n = 64, $p < 0.0001$). Although there is high correlation between $\Delta^{13}C$ and ***RH*** ($r = 0.80$, $n = 63$, $p < 0.001$) during the previous August to October as well as temperature ($r = -0.64$, $n = 63$, $p < 0.001$), the values of the first difference are quite low, being 0.18 and −0.04, respectively. This correlation does not meet the requirements for climate reconstruction.

We, therefore, are more inclined to reconstruct $\boldsymbol{RH}_{\mathbf{AMJ}}$ by the $\Delta^{13}C$ time series, since a change in $\boldsymbol{RH}_{\mathbf{AMJ}}$ is more likely to determine a change in tree ring carbon isotopes at Mt. Tianmu.

Mt. Tianmu is in a subtropical zone, with higher summer temperatures and relatively less summer rainfall from July to September. This pattern results in lower relative humidity during mid-summer (Fig. 4a shows a low in July). The highest relative humidity is in early summer, coinciding with the early growing season of *Cryptomeria fortunei*. We performed analysis of partial correlation among temperature, precipitation, and average relative humidity from April to June. With precipitation held constant, the correlation between $\boldsymbol{RH}_{\mathbf{AMJ}}$ and mean air temperature from April to June is $r = 0.74$ ($p < 0.001$); With temperature held constant, the correlation between $\boldsymbol{RH}_{\mathbf{AMJ}}$ and precipitation from April to June is $r = 0.30$ ($p < 0.05$), indicating that the mean temperature from April to June is the main controlling factor influencing $\boldsymbol{RH}_{\mathbf{AMJ}}$, while precipitation does not exert a significant influence on $\boldsymbol{RH}_{\mathbf{AMJ}}$.

Also, $\delta^{13}C$ variations are linked to the vapor pressure deficit (*VPD*). According to the equation (Castellvi et al. 1997): $VPD = e^*(T_a) - e \approx e^*(T_a)[1 - h_d/100]$, there exists a negative correlation between *VPD* and ***RH***. A decrease in ***RH*** leads to an increase in *VPD*. Thus, $\Delta^{13}C$ would decrease and, ultimately, $\delta^{13}C$ would increase, and vice versa.

5 Results and discussion

According to the analysis above, we designed the following transfer function to carry out a simulated reconstruction of mean relative humidity from April to June at Mt. Tianmu:

$$RH_{\mathbf{AMJ}} = 4.921\Delta^{13}C + 6.655 \quad (3)$$

(n = 64, $r = 0.858$, $p < 0.0001$, $R^2 = 0.737$, $R^2_{adj} = 0.732$, SE = 2.676, $F = 173.336$, $D/W = 1.455$), where $\boldsymbol{RH}_{\mathbf{AMJ}}$ is the mean relative humidity in the growing season from April to June in Mt. Tianmu, and D/W is the determination coefficient of Durbin-Watson. It is observed from the table look-up that when n = 64, D/W lies between 1.41 and 1.47, indicating that the reconstructed equation is free from first-order autocorrelation.

The split-sample method (Meko and Graybill 1995) was used to test the reliability and stability of the reconstructed sequence of $\boldsymbol{RH}_{\mathbf{AMJ}}$. The test requires calculation of a series of statistics, including the sign test (S1, S2), *RE*, and *CE*. If $RE > 0$, the reconstruction is considered to be stable and the reconstructed equation is considered to have passed the test. If $CE > 0$, the result of the reconstruction is considered to be reliable (Liu et al. 2013a).

As the result shows in Table 4, the reconstructed model is reliable and stable. Especially in two different time periods, *CE* is 0.549 (1981–2015) and 0.167 (1951–1985), much higher than zero and the ideal values. The total variance explained (R^2) is 73.7%. Sign test (*ST*) is used to test the similarity between the reconstruction and the observation sequence; product mean (*t*) is used to determine whether the reconstructed and the observed sequences of each year are the same.

Figure 4c shows that the reconstructed sequence tallies with the observed sequence to a great extent, although after the first-order difference, there is still a significant correlation between the two sequences (Fig. 4d, r = 0.56, $p < 0.0001$, n = 63), indicating that our reconstructed sequence has captured the changes characteristic of the observed sequence at both high frequency and low frequency.

Based on Eq. (3), we reconstructed the sequence of $\boldsymbol{RH}_{\mathbf{AMJ}}$ changes at Mt. Tianmu in the period 1648 to 2014 (Fig. 5). We take the mean relative humidity (78.1) from April to June as the mean value for the period 1951 to 2014, $1\sigma = 2.7$. We defined the following: dry year < mean−1σ (75.4), humid year > mean+1σ (80.7), normal year between 75.4 and 80.7. We find that there are 34 dry years (accounting for 9.3% of the total sequence) and 83 humid years (accounting for 22.6% of the total sequence), and the remaining 250 years are normal years (accounting for 68.1% of the total sequence) over the past 367 years. Humid years occurred more frequently than dry years in the Mt. Tianmu region. However, since 1960, a drastically different drying trend occurred. After 1990, dry years increased, and after 2000, the drought intensified with continuously relatively drier years and no humid years.

Our $\boldsymbol{RH}_{\mathbf{AMJ}}$ reconstruction could be well compared to other observed $\boldsymbol{RH}_{\mathbf{AMJ}}$ from different stations (Tianmushan,

Table 4 Statistics of the split calibration-verification model for the mean relative humidity reconstruction

Calibration					Verification						
Period	*r*	R^2	*ST*	*t*	Period	*r*	R^2	*RE*	*CE*	*ST*	*t*
1951–1980	0.461**	0.212	19	4.896**	1981–2014	0.843**	0.711	0.838	0.549	29**	6.020**
1985–2014	0.855**	0.731	27**	6.180**	1951–1984	0.496**	0.246	0.840	0.167	23	5.932**
1951–2014	0.858**	0.737	49**	6.856**	–	–	–	–	–	–	–

*Significant at the 95% confidence level

**Significant at the 99% confidence level

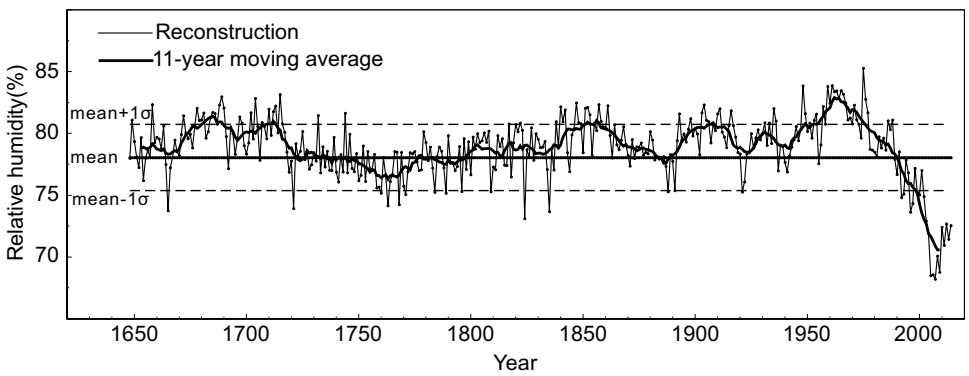

Fig. 5 Reconstructed mean relative humidity series from April to June during the period 1648–2014 AD over Mt. Tianmu. The thick line is an 11-year moving average

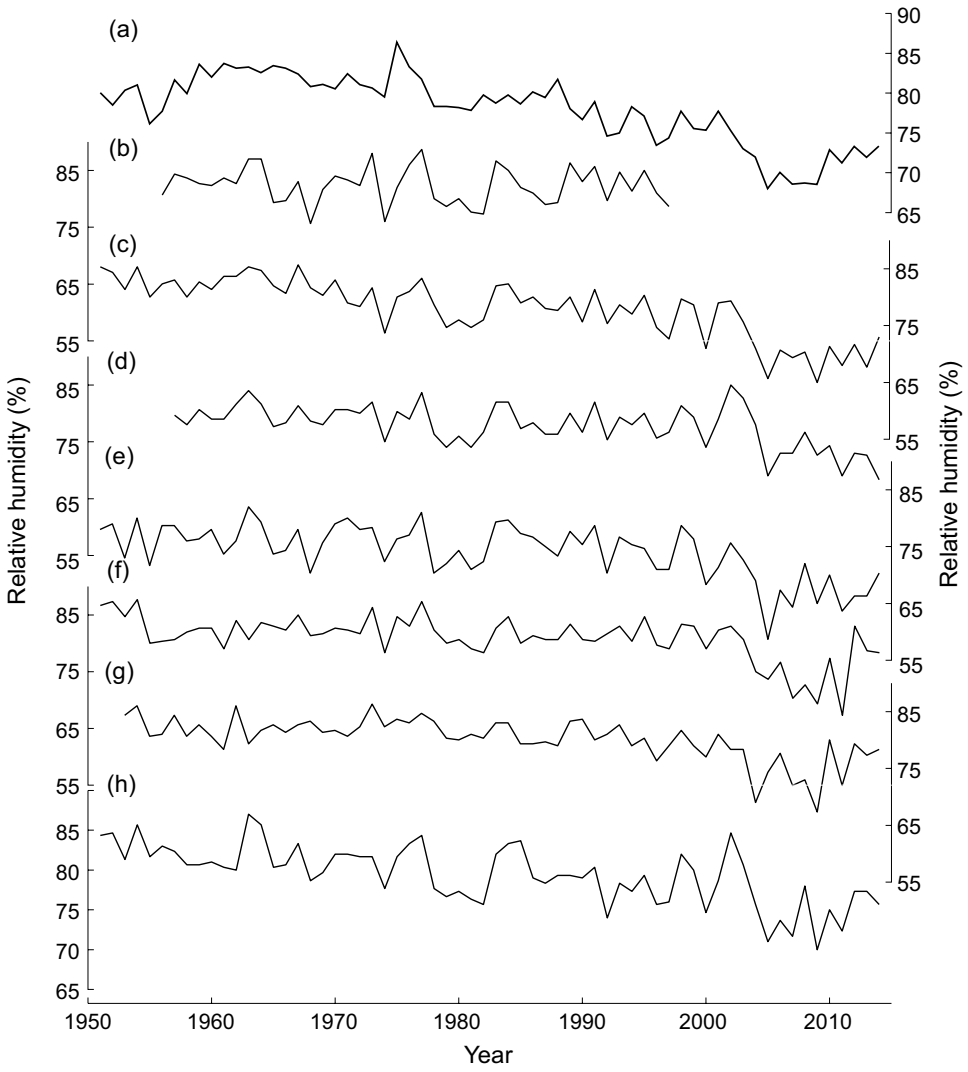

Fig. 6 Comparison within reconstructed (*a*) and observed RH_{AMJ} series from Tianmushan (*b*), Hangzhou (*c*), Ningguo (*d*), Nanjing (*e*), Nanchang (*f*), Fuzhou (*g*), Nantong (*h*)

Hangzhou, Ningguo, Nanjing, Nanchang, Fuzhou, and Nantong). They all displayed synchronous variation trends in RH_{AMJ} (Fig. 6). That is to say, our reconstruction could represent RH_{AMJ} variations on a large scale. It should be noted they all showed a sharply decreasing trend after the 1960s, likely reflecting the weakening of the East Asian summer monsoon since then (Xue et al. 2015).

The spatial correlations were also carried out using the KNMI Climate Explorer (http://climexp.knmi.nl). Calculations show that there is a significant negative correlation between RH_{AMJ} in Mt. Tianmu and SSTs in the western equatorial Pacific Ocean and Indian Ocean (Fig. 7), that is, a negative correlation between the tree ring $\Delta^{13}C$ and SST. Monsoons from the Indian Ocean and western equatorial Pacific Ocean transfer heat to southern China, due to seasonal temperature increases in the tropics. The negative correlation between temperature and relative humidity observed for Mt. Tianmu ($r = -0.76$, $n = 64$, $p < 0.0001$), means that as relative humidity decreases, tree ring $\delta^{13}C$ values increase, and vice versa.

Calculations show that there is a positive correlation between either the observed or reconstructed RH_{AMJ} and the monsoon index of East Asia and South Asia from 1951 to 2014 (Table 5). This is consistent with the spatial correlation shown in Fig. 7. Since Mt. Tianmu is near the western Pacific Ocean, the influence of the East Asian summer monsoon on the region is stronger than the influence of the South Asian monsoon, showing that the reconstructed sequence of RH_{AMJs} and the sequence of EASM by Guo are consistent with each other in terms of interannual changes and overall trends (Fig. 8). When the Asian summer monsoon is stronger, the RH_{AMJ} value is higher; when the Asian summer monsoon becomes weaker, the RH_{AMJ} value is lower.

From this point of view, the key information conveyed to us by Fig. 5 is that since 1960, Asian Summer

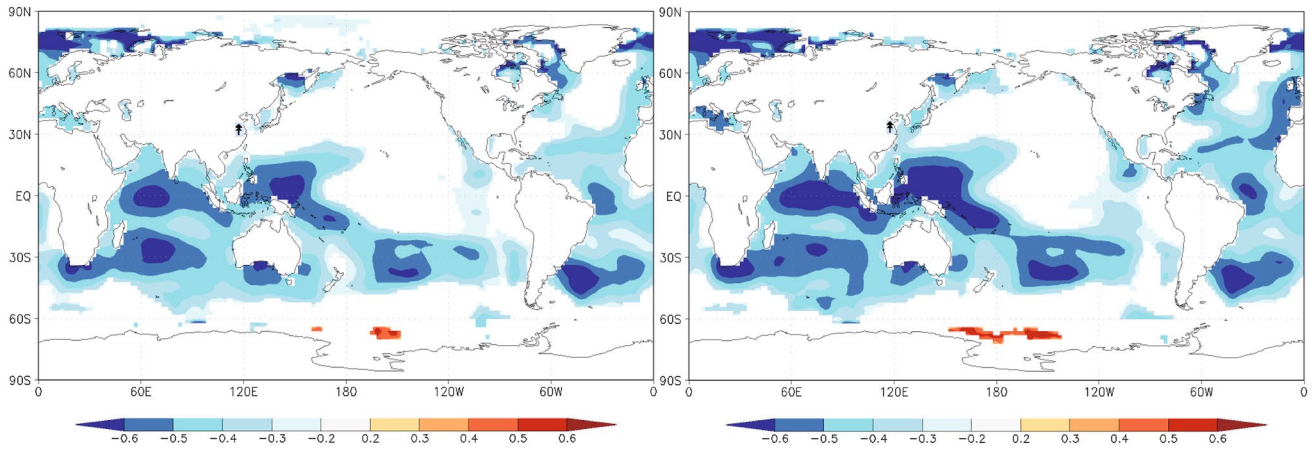

Fig. 7 Spatial correlation map with ERSST v4 SST 1951–2014 ($p < 0.05$). **a** Observation, **b** reconstruction

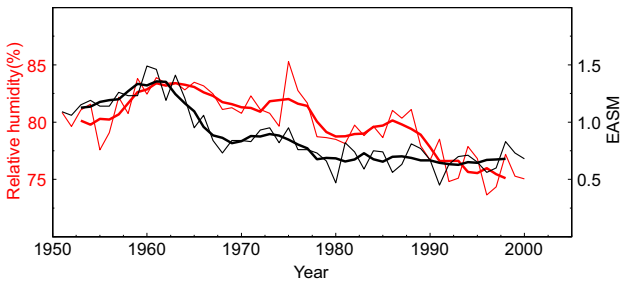

Fig. 8 Comparison between reconstructed mean relative humidity (*red line*) and the East Asian Summer monsoon (*black line*) (Guo 1983). *Thick lines* are 5–year moving averages. The intensity of the summer monsoon was defined by the pressure gradient between the land and sea from 10°N–50°N, 110°E–50°E (Guo 1983)

monsoons have been on the decline, in particular East Asian summer monsoon. This conclusion is consistent with previous research findings (Guo 1983; Liu et al. 2013a, b, 2017a; Li et al. 2015), and the declining trend is consistent with the trend towards global warming, because global warming weakens the Asian Summer monsoons (Yang et al. 2015). However, we also find that relative humidity on Mt. Tianmu started to increase after 2003, which suggests a possible rebound in the Asian Summer monsoon for about the last decade.

$\boldsymbol{RH}_{\mathbf{AMJ}}$ in the Mt. Tianmu area and mean relative humidity in Yaoshan (about 800 km away from the northwest of the Mt. Tianmu area), reconstructed by tree ring $\delta^{18}O$ from April to September, compare closely (Table 6; Fig. 9, Liu et al. 2017b). After an 11-year moving average, Mt. Tianmu and Yaoshan are similar in terms of the changes in relative humidity from 1839 to 1953. However, the 2 curves diverge from 1953 to 1980, likely because Mt. Tianmu is closer to the Pacific Ocean moisture source and, hence, more water vapor. After 1990, the 2 curves again decline along a similar trend, reflecting the weakening of the Asian Summer monsoon at that time.

The reconstruction is synchronous with ***RH*** of Yaoshan, which implies that the climatic response between the carbon isotope of tree rings and ***RH*** was stable through the past 350 years.

6 Conclusions

We selected five *Cryptomeria fortunei* specimens from the Mt. Tianmu to reconstruct relative humidity in southern China. The relation between tree ring $\delta^{13}C$ and climate are examined closely by means of strict dendrochronological methods. After normalizing the influence of atmospheric CO_2, we observed a robust correlation between $\Delta^{13}C$ in our composite tree ring time series and $\boldsymbol{RH}_{\mathbf{AMJ}}$ in the growing season, with correlations of up to $r = 0.86$ ($n = 64$, $p < 0.0001$). We used the $\Delta^{13}C$ composite time series to reconstruct $\boldsymbol{RH}_{\mathbf{AMJ}}$ at Mt. Tianmu for more than 300 years. We find that in the Mt. Tianmu region, the mean

Table 5 Statistical correlation between mean relative humidity on Mt. Tianmu and the East and South Asian monsoon indices

	Period	Observed RH_{AMJ}	Reconstructed RH_{AMJ}
East Asia monsoon index (Li and Zeng 2003)	1951–2014, June–July	0.23, $p < 0.07$	0.28, $p < 0.03$
East Asia monsoon index (Guo 1983)	1951–2000	0.59, $p < 0.0001$	0.62, $p < 0.0001$
South Asia monsoon index (Li and Zeng 2003)	1951–2014, June–August	0.37, $p < 0.003$	0.28, $p < 0.03$

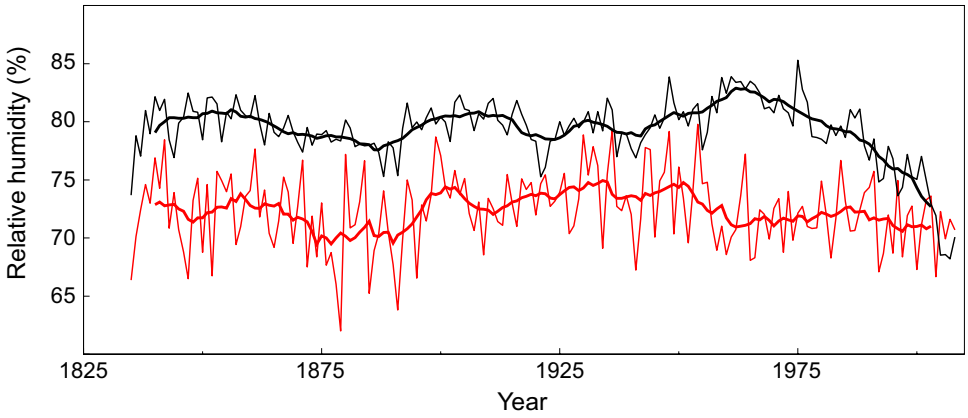

Fig. 9 Comparison of reconstructed mean relative humidity between Mt. Tianmu (from April to June) (*black line*) and Yaoshan (from April to September) (*red line*), 11-year moving average (*thick lines*)

Table 6 Statistical correlation of reconstructed mean relative humidity between Mt. Tianmu (from April to June) and Yaoshan (from April to September)

	1835–1953 AD	1835–2008 AD
Original series	$r=0.29$, $p<0.001$	$r=0.20$, $p<0.01$
11-year moving average	$r=0.48$, $p<0.1$, $df=11$	$r=0.29$, $df=16$

temperature from April to June is the main controlling factor for change in $\boldsymbol{RH}_{\mathbf{AMJ}}$, while precipitation shows minor correlation with $\boldsymbol{RH}_{\mathbf{AMJ}}$.

The reconstructed $\boldsymbol{RH}_{\mathbf{AMJ}}$ also showed positive correlations with both the East Asian and South Asian summer monsoon indices in the period 1951 to 2014, indicating that $\boldsymbol{RH}_{\mathbf{AMJ}}$ in Mt. Tianmu reflects changes in the Asian Summer monsoon intensity to a great extent. The results also show a strong similarity with the Yaoshan site, reconstructed based on tree ring $\delta^{18}O$. In particular, after computing 11-year moving averages, the growth season sequences showed simultaneous variations from 1839 to 1953 and during a common decline in relative humidity after 1990, concurrent with a persistent decline in the Asian Summer monsoon and an increase in global warming.

It is no doubt this research could provide useful information about climate variation in the past in the sub-tropical region of southern China, where a high-resolution proxy is still lacking. To better understand Asian monsoon behavior, more and longer ***RH*** reconstructions are needed in the future.

Acknowledgements We thank Huimin Zhang, Baoyin Shen, Boyang Zhao, George S. Burr and the Mt. Tianmu Nature Reserve Area Management Bureau for their help. This study was jointly supported by Grants from the NSFC41630531, CAS Key Research Program of Frontier Sciences QYZDJ–SSW–DQC021, NSFC41371221, the National Basic Research Program 2013CB955903, NSFC41671212, the CAS "Light of West China" Program, the Key Project of IEECAS and the SKLLQG.

References

An ZS, Zhang PZ, Wang EQ, Wang SM, Qiang XK, Li L, Song Y G, Chang H, Liu XD, Zhou WJ, Liu WG, Cao JJ, Li XQ, Shen J, Liu Y, Ai L (2006) Changes of the monsoon-arid environment in China and growth of the Tibetan plateau since the Miocene. Quat Sci 26 (5) :678–693

Castellvi F, Perez PJ, Stockle CO, Ibaiiez M (1997) Methods for estimating vapor pressure deficit at a regional scale depending on data availability. Agric For Meteorol 87:243–252

Cook ER, Kairiukstis LA (1990) Methods of dendrochronology. Kluwer, Dordrecht, pp 1–397

Cook ER, Anchukaitis KJ, Buckley BM, D'Arrigo RD, Jacoby GC, Wright WE (2010) Asian monsoon failure and megadrought during the last millennium. Science 328(5977):486–489

Coplen TB (1995) Discontinuance of SMOW and PDB. Nature 375:285

Easterling DR, Peterson TC (1995) A new method for detecting and adjusting for undocumented discontinuities in climatological time series. Int J Climatol 15:369–377

Farquhar GD, O'Leary MH, Berry JA (1982) On the relationship between carbon isotope discrimination and the intercellular carbon dioxide concentration in leaves. Aust J Plant Phys 9: 121–137

Freyer HD (1979) $\delta^{13}C$ record in tree rings.1. $\delta^{13}C$ variations in northern hemispheric trees during the last 150 years. Tellus 31:124–137

Gagen MH, Finsinger W, Wagner-Cremer F, McCarroll D, Loader N, Robertson I, Jalkanen R, Young GHF, Kirchhefer A (2011) Evidence of changing intrinsic water-use efficiency under rising atmospheric CO_2 concentrations in Boreal Fennoscandia from subfossil leaves and tree ring $\delta^{13}C$ ratios. Glob Change Biol 17:1064–1072

Guo QY (1983) The summer monsoon intensity index in East Asia and its variation. Acta Geograph Sin 38:207–217 **(in Chinese)**

Hou AH, Peng SL, Zhou GY, Wen DZ (2001) A quantitative explanation of the juvenile effects of tree-ring $\delta^{13}C$. Acta Ecol Sin 21(3):430–433 **(in Chinese)**

Jiang WW, Yang GY, Zhao MS, Yang SZ (2012) Diurnal and seasonal variation of stem sap flow for *Cryptomeria fortunei* in Mount Tianmu. J Nanjing For Univ 36(5):77–80

Jones PD, Mann ME (2004) Climate over past millennia. Rev Geophys 42(2):RG2002

Leavitt SW, Long A (1984) Sampling strategy for stable carbon isotope analysis of tree in pine. Nature 311(13):145–147

Leavitt SW, Long A (1989a) The atmospheric $\delta^{13}C$ record as derived from 56 pinyoa trees at 14 sites in the southwestern tree rings. Water Resources Bull 25:341–347

Leavitt SW, Long A (1989b) Drought indicated in C-13-C-12 ratios of southwestern tree rings. Water Res Bull 25(2):341–347

Leavitt SW, Treydte K, Liu Y (2010) Environment in time and space: opportunities from tree-ring isotope networks. In: JB West (eds) Isoscapes: understanding movement, pattern, and process on earth through isotope mapping. Springer, Dordrecht, pp 113–135

Li Q, Liu Y, Nakatsuka T, Song HM, McCarroll D, Yang YK, Qi J (2015) The 225-year precipitation variability inferred from tree-ring records in Shanxi Province, the North China, and its teleconnection with Indian summer monsoon. Glob Planetary Change 132:11–19

Li JP, Zeng QC (2003) A new monsoon index and the geographical distribution of the global monsoons. Adv Atmos Sci 20(2):299–302

Liu Y, Wu XD, Leavitt SW, Hughes MK (1996) Stable carbon isotope in tree rings from Huangling, China, and climatic variation. Sci China Ser (D) 39:152–161

Liu XH, Qin DH, Shao XM, Zhao LJ, Chen T, Ren JW (2003) Variation and abrupt change of precipitation in Nyingchi Prefecture of Tibet autonomous region in past 350 years. J Glaciol Geocryol 25(4):375–379

Liu Y, Ma LM, Leavitt SW, Cai QF, Liu WG (2004) A preliminary seasonal precipitation reconstruction from tree-ring stable carbon isotopes at Mt. Helan, China, since AD 1804. Glob Planet Change 41:229–239

Liu XH, Shao XM, Wang LL, Zhao LJ, Wu P, Chen T, Qin DH, Ren JW (2007) Climatic significance of the stable carbon isotope composition of tree-ring cellulose: comparison of Chinese hemlock (Tsuga chinensis Pritz) and alpine pine (Pinus densata Mast) in a temperate-moist region of China. Sci China Ser (D) 50:1076–1085

Liu Y, Cai QF, Liu WG, Yang YK, Sun JY, Song HM, Li XX (2008) Monsoon precipitation variation recorded by tree-ring $\delta^{18}O$ in arid Northwest China since AD 1878. Chem Geol 252:56–61

Liu Y, Lei Y, Song HM, Bao G, Sun B, Linderhoim HW, Wang SG (2010a) The annual mean lowest temperature reconstruction based on Pinus Bungeanas (*Pinus bungeana Zucc*.) ring width in the Yulin region, Shandong, China since AD 1616. J Earth Environ 1(1):28–35

Liu XH, An WL, Liang EY, Wang WZ, Shao XM, Huang L, Qin DH (2010b) Spatio-temporal variability and climatic significance of tree ring's $\delta^{13}C$ of picea crassifolia on the Qilian mountains. J Glaciol Geocryol 32(4):666–676

Liu Y, Wang RY, Leavitt SW, Song HM, Linderhoim HW, Li Q, An ZS (2012a) Individual and pooled tree-ring stable-carbon isotope series in Chinese pine from the Nan Wutai region, China: common signal and climate relationships. Chem Geol 330:17–26

Liu Y, Xiang N, Song HM (2012b) Tree-ring temperature records in Arxan, Inner Mongolia for the past 187 years. J Earth Environ 3(3):862–867. doi:10.7515/JEE201203003 **(Chinese)**

Liu Y, Lei Y, Sun B, Song HM, Li Q (2013a) Annual precipitation variability inferred from tree-ring width chronologies in the Changling–Shoulu region, China, during AD 1853–2007. Dendrochronologia 31:290–296. doi:10.1016/j.dendro.2013.02.001

Liu Y, Sun B, Song HM, Lei Y, Cai QF (2013b) Tree-ring-based precipitation reconstruction for Mt. Xinglong, China, since AD 1679. Quat Int 283:46–54

Liu Y, Wang YC, Li Q, Song HM, Linderhoim HW, Leavitt SW, Wang RY, An ZS (2014) Tree-ring stable carbon isotope-based May–July temperature reconstruction over Nanwutai, China, for the past century and its record of 20th century warming. Quat Sci Rev 93:67–76

Liu Y, Zhang YH, Cai QF, Song HM, Ma YY, Mei RC (2015) The tree-ring width based seasonal minimum temperature reconstruction at Shiren Mountains, Henan, China since 1850 AD and its record of 20th century warming. J Earth Environ 6(6):393–406. doi:10.7515/JEE201506003

Liu Y, Zhang XJ, Song HM, Cai QF, Li Q, Zhao BY, Liu H, Mei RC (2017a) Tree-ring-width-based PDSI reconstruction for central Inner Mongolia, China over the past 333 years. Clim Dyn 48(3–4): 867–879

Liu Y, Liu H, Song HM, Li Q, George SB, Wang L, Hu SL (2017b) A 174-year Asian summer monsoon related relative humidity record from tree-ring $\delta^{18}O$ in the Yaoshan region, eastern central China. Sci Total Environ 593/594: 523–534

Loader NJ, Walsh RPD, Robertson I, Bidin K, Ong RC, Reynolds G, McCarroll D, Gagen M, Young GHF (2011) Recent trends in the intrinsic water-use efficiency of ringless rainforest trees in Borneo. Philos Trans R Soc b-Biol Sci 366(1582):3330–3339

Mann ME, Zhang ZH, Hughes MK, Bradley RS, Miller SK, Rutherford S, Ni FB (2008) Proxy-based reconstructions of hemispheric and global surface temperature variations over the past two millennia. Proc Natl Acad Sci 105:13252–13257

McCarroll D, Loader NJ (2004) Stable isotopes in tree rings. Quat Sci Rev 23(7–8):771–801

McCarroll D, Gagen MH, Loader NJ, Robertson I, Anchukaitis KJ, Los S, Young GHF, Jalkanen R, Kirchhefer A, Waterhouse JS (2009) Correction of tree ring stable carbon isotope chronologies for changes in the carbon dioxide content of the atmosphere. Geochim Cosmochim Acta 73:1539–1547

Meko DM, Graybill DA (1995) Tree-ring reconstruction of upper Gila River discharge. Water Res Bull 31(4): 605–616

Peterson TC, Easterling DR (1994) Creation of homogeneous composite ciimatoiogical reference series. Int J Climatol 14:671–679

Porter TJ, Pisaric MFJ, Field RD, Kokeli SV, Edwards TWD, Montigny P, Healy R, LeGrande AN (2014) Spring-summer temperatures since AD 1780 reconstructed from stable oxygen isotope ratios in white spruce tree-rings from the Mackenzie Delta, northwestern Canada. Clim Dyn 42:771–785

Potter KW (1981) Illustration of a new task for detecting a shift mean precipitation series. Mon Weather Rev 109:2040–2045

Qian JL, Lv J, Tu QP, Wang SM (2002) Reconstruction of the climate in the Tianmu Mountain area, Zhejiang Province, in the last 160 years by $\delta^{13}C$ sequence of tree ring α-cellulose. Sci China Ser (D) 45(5):409–419

Sano M, Buckley BM, Sweda T (2009) Tree-ring based hydroclimate reconstruction over northern Vietnam from Fokienia hodginsii: eighteenth century mega-drought and tropical Pacific influence. Clim Dyn 33(2–3):331–340

Saurer M, Borella S, Schweingruber F, Siegwolf R (1997) Stable carbon isotopes in tree rings of beech: climatic versus site-related influences. Trees Struct Funct 11: 291–297

Stokes MA, Smiley TL (1996) An introduction to tree-ring dating. The University of Arizona Press, Tucson, pp 1–73

Stuiver M, Braziunas T (1987) Tree cellulose $^{13}C/^{12}C$ isotopic ratios and climatic change. Nature 328:58–60

Szymczak S, Joachimski MM, Bräuning A, Hetzer T, Kuhlemannd J (2012) Arepooled tree ring $\delta^{13}C$ and $\delta^{18}O$ series reliable climate archives—a case study of Pinus nigra spp. laricio (Corsica/France). Chem Geol 40–49

Treydte KS, Frank DC, Saurer M, Helle G, Schleser GH, Esper J (2009) Impact of climate and CO_2 on a millennium-long tree-ring carbon isotope record. Geochim Cosmochim Acta 73(16):4635–4647

Wang YJ, Chen FH, Gou XH (2001) Reconstruction of spring precipitation in the middle region of the Qilian Mountains using tree-ring data. Sci Geogr Sin 21(4):373–377 **(in Chinese)**

Xu GB, Liu XH, Qin DH, Chen T, An WL, Wang WZ, Wu GJ, Zeng XM, Ren JW (2013) Climate warming and increasing atmospheric CO_2 have contributed to increased intrinsic water-use efficiency on the northeastern Tibetan Plateau since 1850. Trees 27:465–475

Xu CX, Ge JY, Nakatsuka T, Yi L, Zheng HZ, Sano M (2016) Potential utility of tree ring $\delta^{18}O$ series for reconstructing precipitation records from the lower reaches of the Yangtze River, southeast China. J Geophys Res Atmos 121:3954–3968. doi:10.1002/2015JD023610

Xue F, Zeng QC, Huang RH, Li CY, Lu RY, Zhou TJ (2015) Recent advances in monsoon studies in China. Adv Atmos Sci 32:206–229

Yang SL, Ding ZL, Li YY, Wang X, Jiang WY, Huang XF (2015) Warming-induced northwestward migration of the East Asian monsoon rain belt from the Last Glacial Maximum to the mid-Holocene. Proc Natl Acad Sci 112(43):13178–13183

Zhao XY, Wang J, Qian JL (2005) Analysis on the commonness and individuality of the $\delta^{13}C$ annual series of tree rings at Tianmu Mountain. Geogr Geo-Inf Sci 21(4):104–108 **(in Chinese)**

Zhao XY, Zheng ZW, Shang ZY, Wang J, Cheng RQ, Qian JL (2014) Climatic information recorded in stable carbon isotopes in tree rings of *Cryptomeria fortunei*, Tianmu Mountain, China. Dendrochronologia 32(3):256–265